The 9th International Symposium on Automation and Robotics in Construction June 3-5, 1992 Tokyo, Japan

APPLICATION HEIGHT CONTROL SYSTEM OF A TRACTOR CARRYING UP WEAK SLOPE AT DRIVING STATE

TATSURO MURO
Prof. Department of Civil and Ocean Engineering
Faculty of Engineering, Ehime University
3 Bunkyo-cho, Matsuyama, 790, JAPAN

ABSTRACT

When a tractor is carrying up a scraper under transportation of soil on a weak slope, the application height of the effective driving force of the tractor could be controlled to obtain the maximum drawbar pull. Several tractive performances of a 50 kN flexible rubber tracked vehicle trailing up a given weak sandy slope terrain of Cone Index 95 kPa have been simulated. As the results, it is clarified that the optimum application height of the drawbar pull to take the maximum optimum effective driving force of the tractor carrying up the weak sandy slope terrain of 0, $\pi/18$, $\pi/9$ and $\pi/6$ rad results in about 60, 60, 20 and -40 cm for the vehicle eccentricity 0.00, respectively. Then, the automated control system of the optimum application height should be considered in accordance with the tractive effort jointed to the scraper.

1. INTRODUCTION

At earth moving site in highway construction, the position of applied forces of the drawbar pull to a tractor trailing up a scraper on a weak slope terrain influences predominantly the relations between driving force, effective driving force, sinkage, vehicle trim angle, eccentricity of resultant normal force, and slip ratio. Also, the flexibility of a rubber track belt affects the shape of contact pressure distribution and it is dominant not only over the thrust but over the amount of slip sinkage at the rear sprocket.

The purpose of this study is to verify the traffic performances of a flexible tracked vehicle carrying up a weak sandy slope terrain at driving state for establishing the fundamental application height control system of the tractor.

Here, several tractive performances of 50 kN weight, 320 cm track length and 25 cm track width tractor trailing up a scraper on the weak sandy slope terrain of 95 kPa Cone Index and the given terrain-track system constants have been analysed by use of the simulation program which predicts the method of the optimum effective driving force determination from the thrust developed on the interface between track belt and slope terrain and the locomotion resistance and the inclined vehicle weight etc.. Afterwards, several relations between the application height of the effective driving force on the tractor and tractive performance are verified for various slope angles and vehicle eccentricities. Then some positioning system of the attachment of tractor to the optimum application height could be presented by use of some drawbar pull or torque sensor and rut depth sensor, etc..

2. TERRAIN-TRACK SYSTEM CONSTANTS

Fig.1 shows the flexible track model plate of which the grouser height H is 6.5 cm, the pitch G_p is 14.6 cm and the grouser shape is an equilateral trapezoid of $\alpha = \pi/6$ rad, contact length $L=2$ cm [1]. The dimensions of track model is the length $D=73$ cm, the width $B=25$ cm. And the track belt is made of natural rubber of spring hardness 62. The weak terrain is composed of a loose sandy soil of which the bulk density is 1.44 Mg/m^3, the water content is 2.38 %, the relative density is 44.0 %, the average grain size is 0.78 mm, the coefficient of uniformity is 12.0, and the Cone Index is 95.1 kPa.

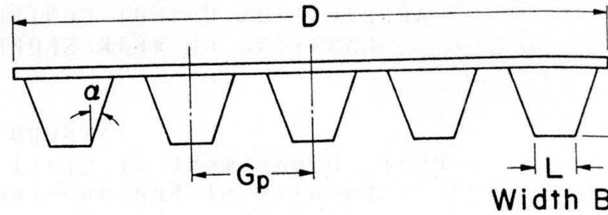

Fig.1 Track model plate and shape of rubber grouser

To predict the interaction between track plate and terrain, next experimental equations could be presented :

$$p = k_1 s_0^{n_1} \qquad (1)$$

$$p = k_1 s_p^{n_1} - k_2 (s_p - s_0)^{n_2} \qquad (2)$$

for track plate loading and reloading test, where p (kPa) is the contact pressure, s_0 (cm) is the amount of static sinkage and s_p (cm) is the static sinkage at the beginning of reloading state.

$$\tau = (m_c + m_f\, p)\{1 - \exp(-a\, j)\} \qquad (3)$$

for track plate traction test, where τ (kPa) is the shear resistance and j (cm) is the amount of slippage of grouser.

$$s_s = c_0\, p^{c_1}\, j_s^{c_2} \qquad (4)$$

for track plate slip sinkage test, where s_s (cm) is the amount of slip sinkage and j_s (cm) is the amount of slippage of soil.

Those ten terrain-track system constants are shown in Table 1.

Table 1 Terrain-track system constants

Static pressure sinkage test	
$k_1 = 8.526$	$k_2 = 32.63$
$n_1 = 0.866$	$n_2 = 0.632$
Shear deformation test	
$m_c = 0$ kPa	$m_f = 0.769$
$a = 0.244$ 1/cm	
Slip sinkage test	
$c_0 = 1.588$	$c_1 = 0.075$
$c_2 = 0.240$	

3. FORCE AND ENERGY BALANCES

Fig.2 shows the vehicle dimensions of tractor and several forces acting on the two track belts carrying up the weak terrain of slope angle β at driving state. From the force balances, the effective driving force T_4 is given as

$$T_4 = \frac{T_3}{\cos\theta_{ti}'} - \frac{W \sin(\theta_{ti}' + \beta)}{\cos\theta_{ti}'} - T_2 \qquad (5)$$

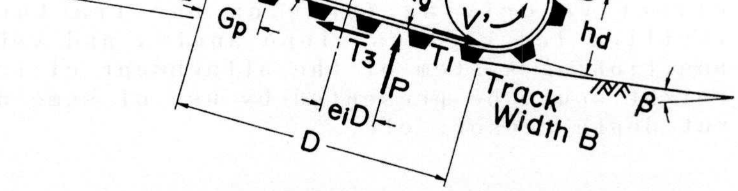

Fig.2 Several forces acting on the two track belts on weak slope terrain at driving state

where T_3' is the thrust [2] acting along the contact part of track belt, T_2 is the land locomotion resistance acting on the front part of undercarriage at depth z. W is the vehicle weight and θ_{ti}' is the trim angle of the vehicle.

The energy balances [3] between effective input energy E_1 supplied by the driving torque $Q=T_1 R_r$ and output energy which is the sum of the compaction energy E_2 to make a rut under the tractor, the slippage energy E_3 developed under the track belt, the effective driving force energy E_4 and the potential energy E_5 are given as follows :

$$E_1 = E_2 + E_3 + E_4 + E_5 \tag{6}$$

where

$$E_1 = T_3 V' \tag{7}$$
$$E_2 = T_2 V'(1-i_d) \tag{8}$$
$$E_3 = T_3\left(1-\frac{1-i_d}{\cos\theta_{ti}'}\right)V' + W V'(1-i_d)\tan\theta_{ti}' \cos\beta \tag{9}$$
$$E_4 = T_4 V'(1-i_d) \tag{10}$$
$$E_5 = W V'(1-i_d)\sin\beta \tag{11}$$
$$i_d = 1-\frac{V}{V'} \tag{12}$$

V is the vehicle speed in the direction of slope terrain surface and V' is the rotation speed of track belt.

4. FLOW CHART

Fig.3 shows the flow chart to calculate the tractive performances of the flexible rubber tracked tractor carrying up the weak slope terrain at driving state. First of all, the vehicle dimensions of the tractor as shown in Table 2 and the terrain-track system constants should be read as input data.

At rest, the relation between contact pressure $p_0(X)$ and amount of sinkage $s_0(X)$ could be calculated from the constants k_1, n_1 and k_2, n_2 [4]. At driving state for a given slip ratio i_d, the resultant normal force P, and the distribution of contact pressure $p_i(X)$ and amount of sinkage $s_i(X)$ of the flexible track belt are repeatedly calculated until the eccentricity e_i is determined, in dependence on the three kinds of flow system. The flexibility of track belt depends on the initial track tension H_0, the ground reaction $p_i(X)$ and shear resistance $\tau_i(X)$, so that the distribution of track tension $T_0(X)$ is given as the summation of H_0 and the thrust which is calculated as

Table 2 Vehicle dimensions

Vehicle weight	W	50 kN
Width of track belt	B	25 cm
Contact length of track belt	D	320 cm
Mean contact pressure	p_m	31.25 kPa
Radius of front idler	R_f	50 cm
Radius of rear sprocket	R_r	50 cm
Radius of track roller	R_m	8 cm
Height of grouser	H	6.5 cm
Grouser pitch	G_p	14.6 cm
Interval of track roller	R_p	40 cm
Eccentricity of gravity center of vehicle	e	− 0.02
Height of gravity center of vehicle	h_g	100 cm
Distance between central axis of vehicle and point acting effective driving force	ℓ_d	300 cm
Height of point acting effective driving force	h_d	60 cm
Initial track tension	H_0	19.6 kN
Rotation speed of track belt at driving state	V'	100 cm/s

the integration of $\tau_i(X)$.

The final values of $T_1 = T_3$, T_4 and e_i, the distributions of amount of slippage $j(X)$, normal pressure $p_i'(X)$, shear resistance $\tau_i'(X)$ [5], amount of sinkage $s_i(X)$ and track belt tension $T_0(X)$, the energies E_1, E_2, E_3, E_4 and E_5, and the tractive efficiency of power E_t [6] can be determined for each slip ratio i_d. And the optimum effective driving force T_{4opt} at the optimum slip ratio i_{dopt} or the maximum effective driving force T_{4max} at the slip ratio i_m can be determined.

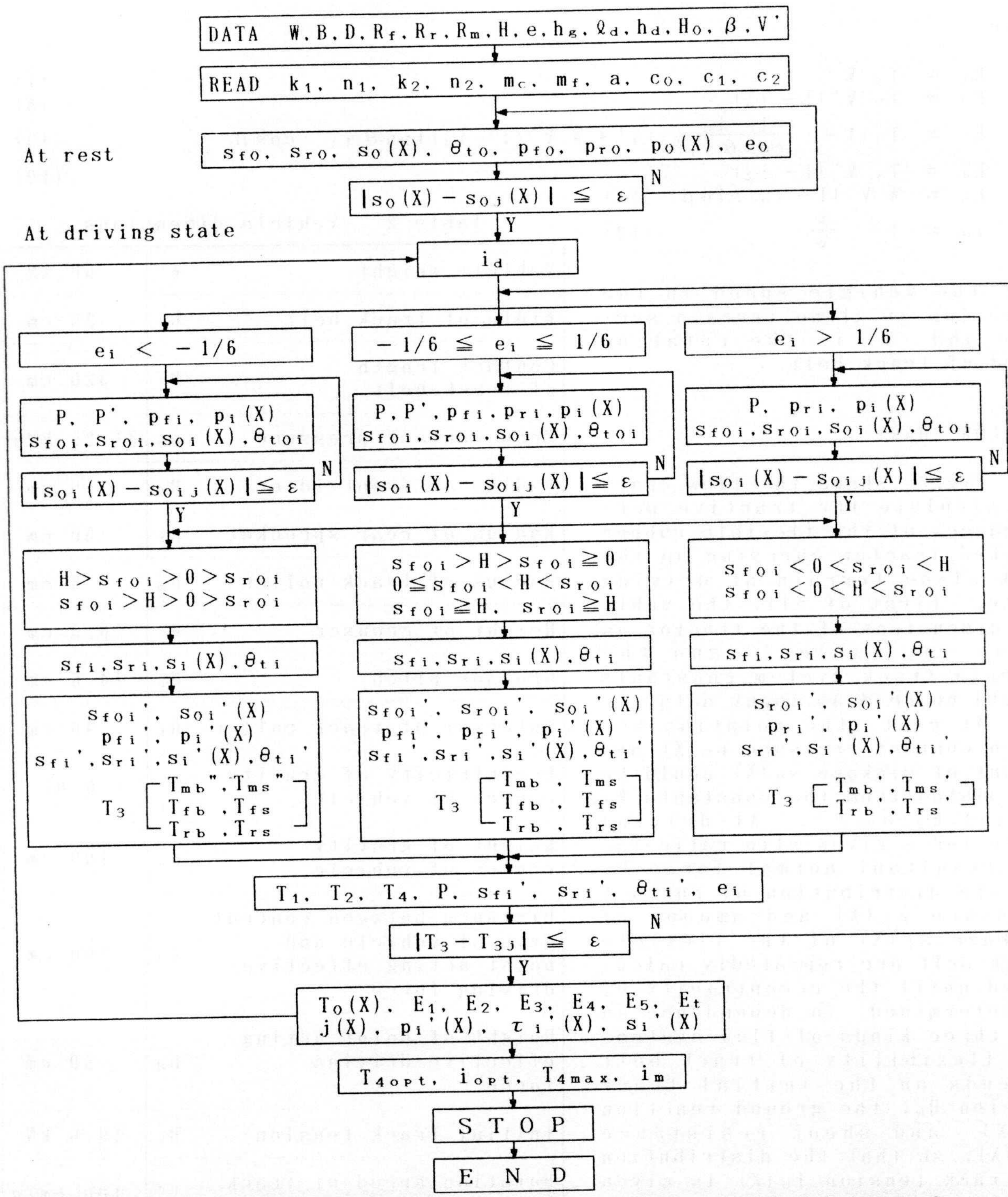

Fig.3 Flow chart to calculate the tractive performances of a flexible tracked tractor carrying up weak slope terrain

5. TRACTIVE PERFORMANCES ON SLOPE

The tractive performances of the given rubber tracked tractor have been simulated for the loose sandy soil of slope angle $\beta = \pi/9$ rad at driving state. The rotation speed of the track belt V' is 100 cm/s and the initial track tension H_0 is 19.6 kN. As shown in Fig.4, the driving force T_1 increases rapidly with i_d at lower slip ratio and does gradually at higher slip ratio, but the effective driving force T_4 decreases gradually with i_d after taking the maximum value $T_{4max} = 20.1$ kN at $i_m = 23$ % due to the increasing locomotion resistance and drops suddenly over $i_d = 90$ %. The optimum effective driving force T_{4opt} is 19.2 kN and the effective driving force energy E_4 reaches the maximum value 1711 kNcm/s at $i_{dopt} = 11$ %, and the tractive efficiency of power E_t is 43.1 %. Fig.5 shows that the amount of sinkage s_{ri}' increases monotonously with i_d and does rapidly over $i_d = 90$ %, and s_{ri}' is always larger than s_{fi}' due to the increasing amount of slip sinkage. Fig.6 shows that the trim angle of vehicle θ_{ti}' increases gradually with i_d, and the eccentricity of resultant normal force e_i decreases gradually after taking the maximum value 0.0384 at $i_d = 6$ % and drops suddenly over $i_d = 90$ %. Fig.7 shows that E_1 increases rapidly with i_d at lower slip ratio and does gradually at higher slip ratio, E_2 and E_4 has a peak value at some slip ratio and reaches zero at $i_d = 100$ % respectively, E_3 increases almost linearly with the increment of i_d, and E_5 decreases linearly

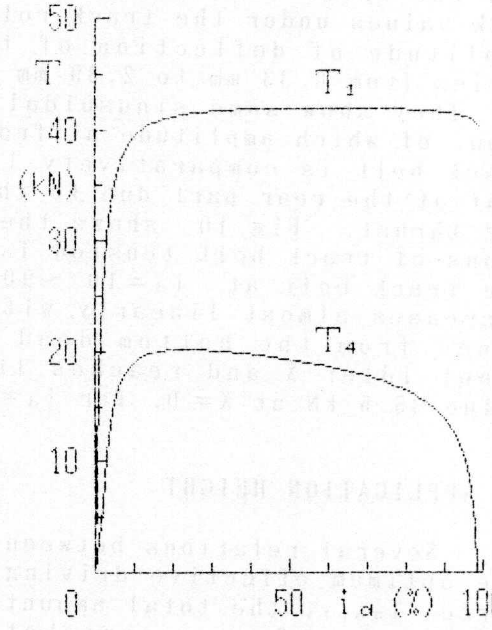

Fig.4 Relations between driving force T_1, effective driving force T_4, and slip ratio i_d ($\beta = \pi/9$ rad)

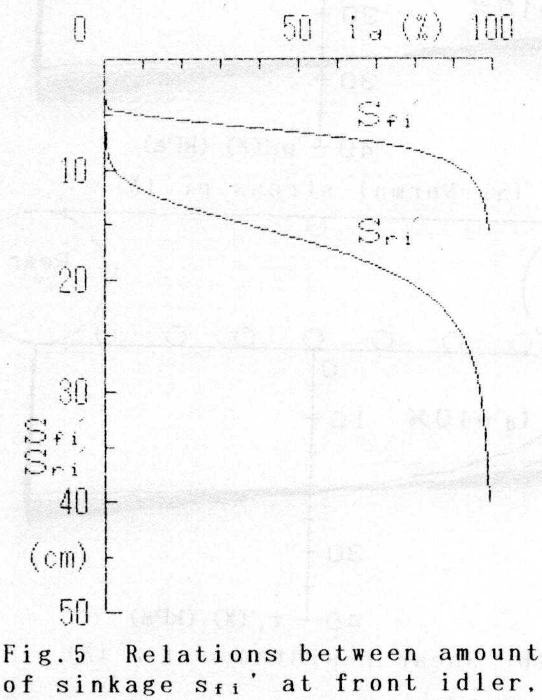

Fig.5 Relations between amount of sinkage s_{fi}' at front idler, s_{ri}' at rear sprocket, and slip ratio i_d ($\beta = \pi/9$ rad)

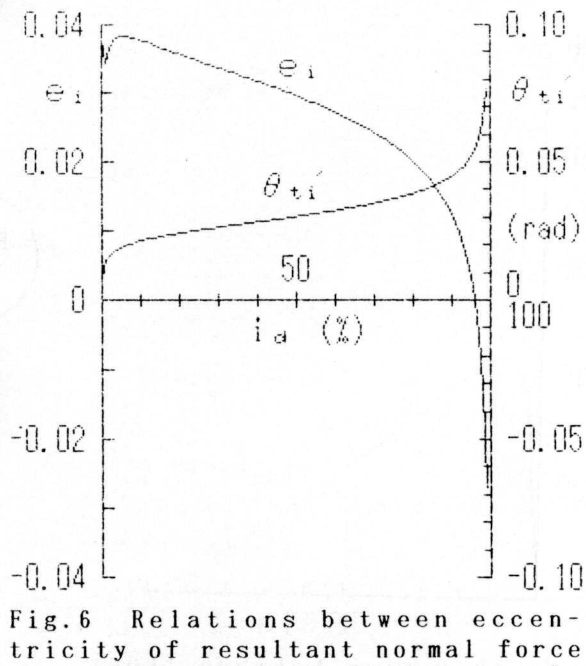

Fig.6 Relations between eccentricity of resultant normal force e_i, trim angle of vehicle θ_{ti}', and slip ratio i_d ($\beta = \pi/9$ rad)

with i_d toward zero at $i_d = 100$ %. Fig.8 shows that the tractive efficiency of power E_t decreases gradually with i_d after taking the maximum value 43.5 % at $i_d = 9$ % and reaches zero at $i_d = 99$ %. Fig.9 shows the contact pressure distribution under the flexible track belt at $i_d = 10 \sim 90$ %, in which the normal stress $p_i'(X)$ and the shear resistance $\tau_i'(X)$ have peak values under the track rollers. The amplitude of deflection of track belt varies from 0.33 mm to 2.39 mm at $i_d = 10$ %. They show some sinusoidal distribution, of which amplitude at front part of track belt is comparatively larger than that at the rear part due to the increasing thrust. Fig.10 shows the distributions of track belt tension $T_0(X)$ around the track belt at $i_d = 10 \sim 90$ %. $T_0(X)$ increases almost linearly with the distance from the bottom dead center of front idler X and reaches the maximum value 35.5 kN at X = D, for $i_d = 10$ %.

6. APPLICATION HEIGHT

Several relations between the optimum effective driving force T_{4opt}, the total amount of sinkage of rear sprocket s_{ri}, the eccentricity of resultant normal force e_i, the trim angle of vehicle θ_{ti}, the tractive efficiency of

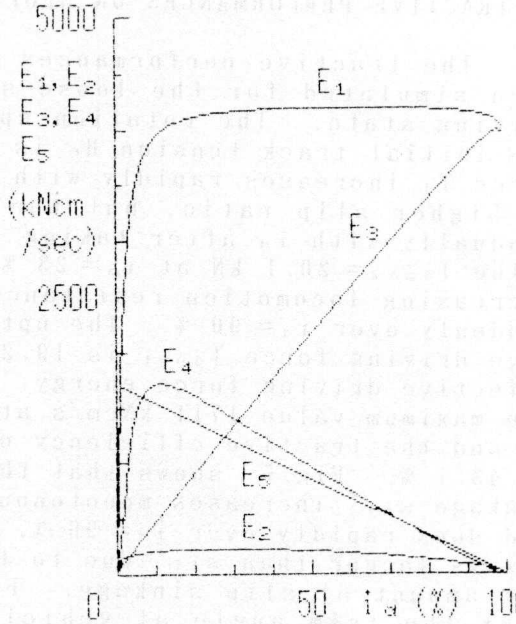

Fig.7 Relations between energy E_1, E_2, E_3, E_4, E_5 and slip ratio i_d ($\beta = \pi/9$ rad)

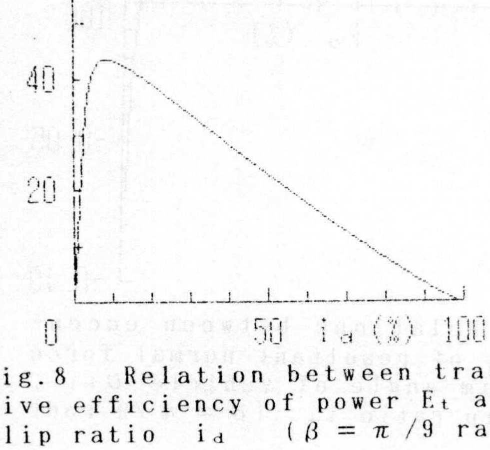

Fig.8 Relation between tractive efficiency of power E_t and slip ratio i_d ($\beta = \pi/9$ rad)

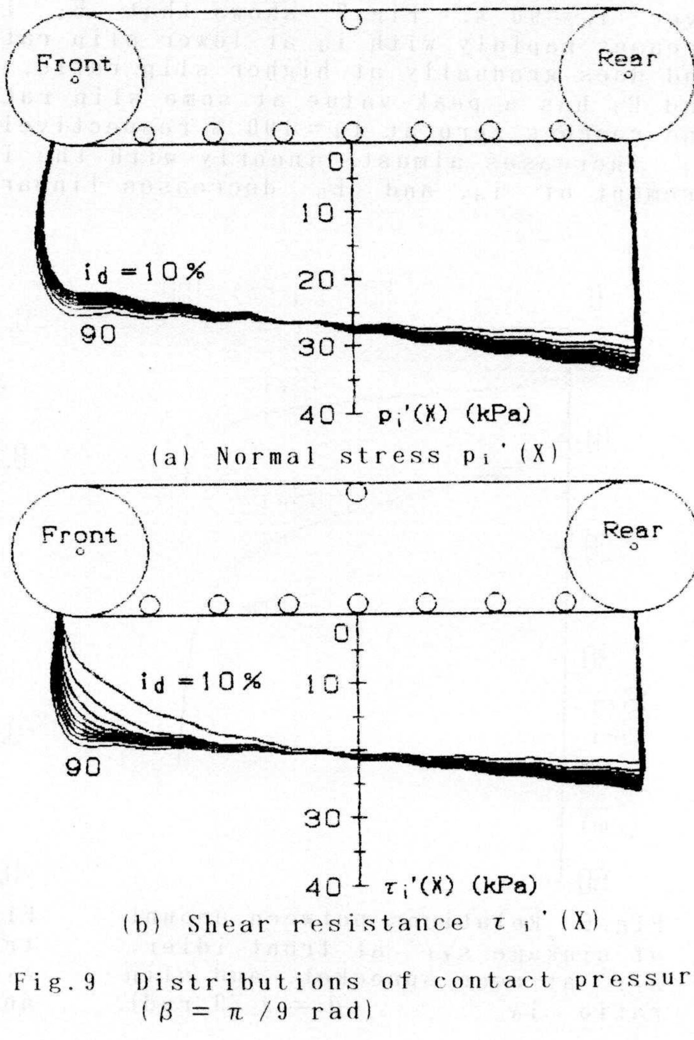

(a) Normal stress $p_i'(X)$

(b) Shear resistance $\tau_i'(X)$

Fig.9 Distributions of contact pressure ($\beta = \pi/9$ rad)

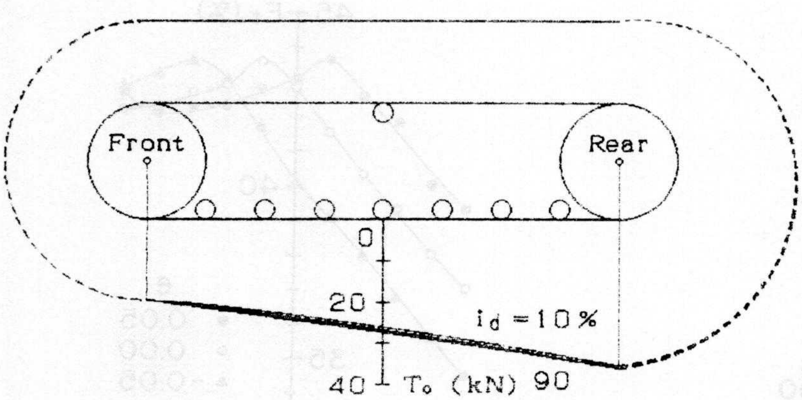

Fig.10 Distributions of track belt tension T_0 around track belt ($\beta = \pi/9$ rad)

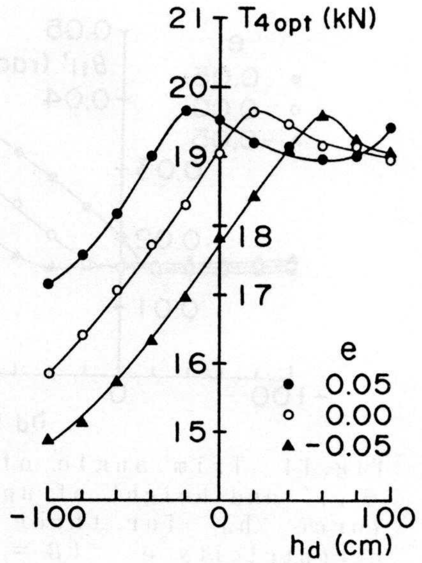

Fig.11 Optimum effective driving force T_{4opt} and height of application force h_d for three kinds of eccentricity e ($\beta = \pi/9$ rad)

power E_t, and the height of point acting effective driving force h_d have been calculated for the loose sandy soil of slope angle $\beta = \pi/9$ rad at driving state and for the same vehicle dimensions except the eccentricity of gravity center of vehicle e = 0.05, 0.00 and −0.05 and h_d = −100 to 100 cm at every 20 cm. Fig.11 shows the relations between T_{4opt} and h_d for the given eccentricities. T_{4opt} takes a maximum value at h_d = −20 cm for e = 0.05, at h_d = 20 cm for e = 0.00, and at h_d = 60 cm for e = −0.05. For a given depth of application of excavating force, the larger the value of eccentricity e the larger the excavating force T_{4opt} that could be obtained. In these cases, the maximum T_{4opt} are less than the half of the vehicle weight W. Fig.12 shows the relations between s_{ri}' and h_d for the given eccentricities : s_{ri}' takes a minimum value at h_d = −20 cm for e = 0.05, at h_d = 20 cm for e = 0.00, and at h_d = 60 cm for e = −0.05. For h_d larger than the height at minimum value of sinkage, s_{ri}' increases gradually with the increment of h_d. However, for h_d less than that, s_{ri}' increases remarkably

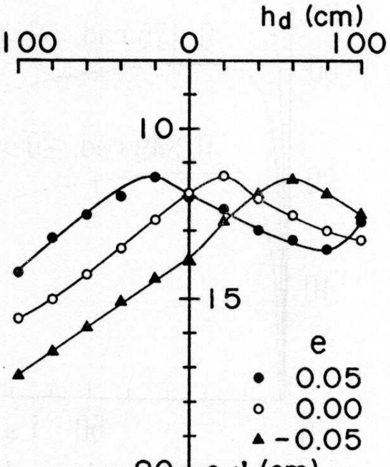

Fig.12 Total amount of sinkage of rear sprocket s_{ri} and height of application force h_d for three kinds of eccentricity e ($\beta = \pi/9$ rad)

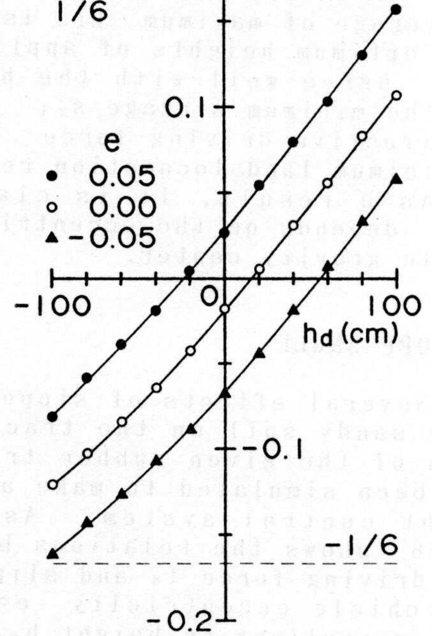

Fig.13 Eccentricity of resultant normal force e_i and height of application force h_d for three kinds of eccentricity e ($\beta = \pi/9$ rad)

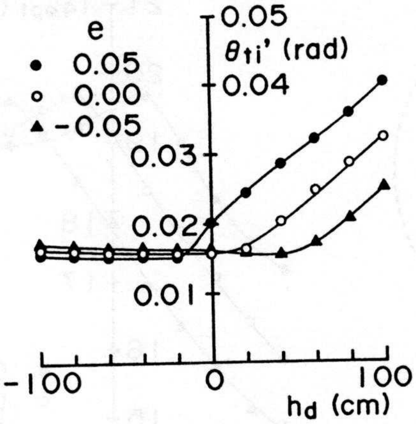

Fig.14 Trim angle of vehicle θ_{ti}' and height of application force h_d for three kinds of eccentricity e ($\beta = \pi/9$ rad)

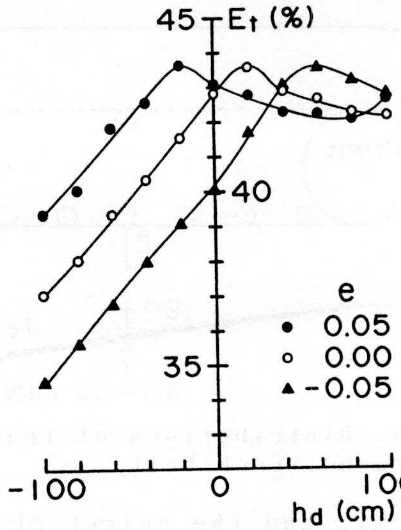

Fig.15 Tractive efficiency of power E_t and height of application force h_d for three kinds of eccentricity e ($\beta = \pi/9$ rad)

with the decrement of h_d due to the negative eccentricity e_i of the resultant normal force. In these cases, the average of minimum amounts of sinkage s_{ri}' is about 11.4 cm depth. Fig.13 shows the relations between e_i and h_d for the given eccentricities. In general, e_i increases monotonously with the increment of h_d. For a given h_d, the larger the eccentricity e, the larger e_i that could be obtained, and every e_i is located within the middle third of the bottom track belt. Fig.14 shows the relations between θ_{ti}' and h_d for the given eccentricities : θ_{ti}' decreases almost linearly with the decrement of h_d and reduces to some value at a large depth of excavation. Fig.15 shows the relations between E_t and h_d for the given eccentricities : E_t takes a maximum value at the optimum application height $h_{dopt} = -20$ cm for $e = 0.05$, at $h_{dopt} = 20$ cm for $e = 0.00$, and at $h_{dopt} = 60$ cm for $e = -0.05$. In these cases, the average of maximum E_t is about 43.6 %. These optimum heights of application force h_{dopt} agree well with the heights which show the minimum sinkage s_{ri}' and the maximum effective driving force T_{4opt}, due to the minimum land locomotion resistance.

As a result, it is clarified that h_{dopt} depends on the eccentricity e of the vehicle gravity center.

7. SLOPE ANGLE

Several effects of slope angle of the loose sandy soil on the tractive performances of the given rubber tracked tractor have been simulated to make an application height control system. As an example, Fig.16 shows the relations between effective driving force T_4 and slip ratio i_d for the vehicle eccentricity $e = 0.00$, at the optimum application height $h_{dopt} = 60$ cm for the slope angle $\beta = 0$ rad, at $h_{dopt} = 60$ cm for $\beta = \pi/18$ rad, and at $h_{dopt} = 20$ cm for $\beta = \pi/9$ rad, respectively. Fig.17 shows the relations between total amount of

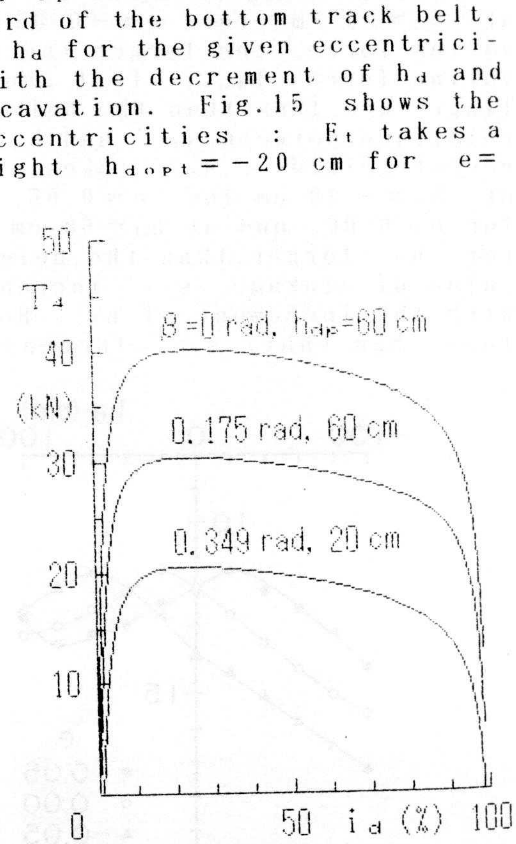

Fig.16 Effective driving force T_4 and slip ratio i_d for various slope angles β and optimum application heights h_{dopt} ($e = 0.00$)

sinkage of rear sprocket s_{ri}' and slip ratio i_d in correspondence with the same vehicle dimensions and slope angle, respectively.

In general, the optimum effective driving force T_{4opt} decreases remarkably with the increment of slope angle β due to the increasing vehicle weight component $W\sin(\theta_{ti}'+\beta)/\cos\theta_{ti}$ in Eq(5), while the $s_{ri}'-i_d$ curve has almost the same relationship as shown in Fig.17 for various β values.

The optimum application height h_{dopt} to maximize the effective driving force and the tractive power efficiency at the optimum slip ratio depends on the eccentricity of gravity center of the vehicle e and the slope angle β. As shown in Fig.18, h_{dopt} decreases with the increment of e and β, and then the positioning system of the attachment of tractor to h_{dopt} could be developed by use of some inclinometer to measure the slope angle β of the running terrain.

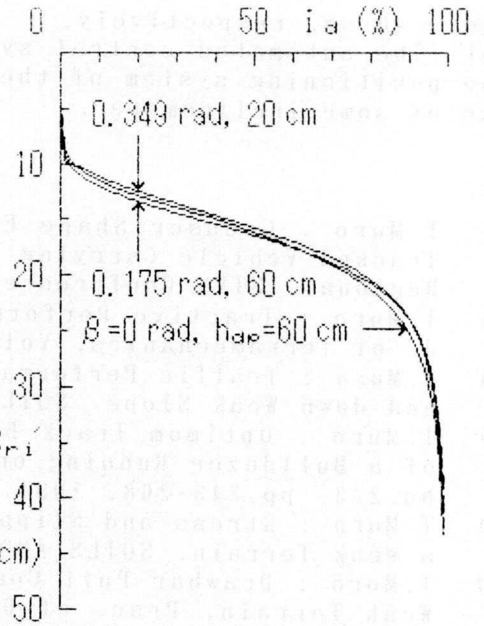

Fig.17 Total amount of sinkage of rear sprocket s_{ri}' and slip ratio i_d for various slope angles β and optimum application heights h_{dopt} (e= 0.00)

8. CONCLUSIONS

To establish an optimum operation and robotization system of a flexible rubber tracked tractor carrying up weak slope terrain, some application height control system to obtain the maximum drawbar pull should be considered. Here, several tractive performances of a 50 kN weight tractor carrying up a loose sandy soil slope terrain have been simulated for various slope angles and vehicle eccentricities to find the optimum application height by use of the given terrain-vehicle constants. As the results, it is clarified that :

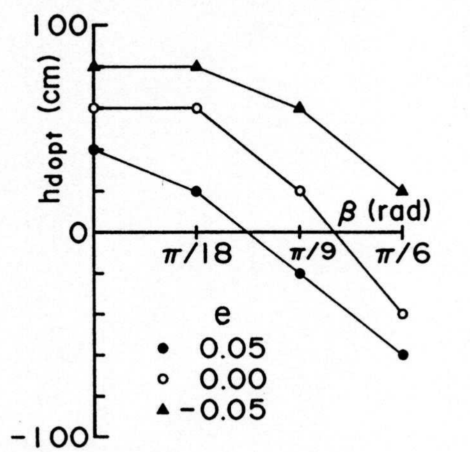

Fig.18 Relations between optimum application height h_{dopt} and slope angle β for three kinds of eccentricity e

(1) The optimum height of application of effective optimum drawbar pull to obtain the maximum value agrees well with the height, at which the amount of sinkage of rear sprocket takes a minimum value and the tractive efficiency of power takes a maximum value.

(2) For the slope angle $\pi/9$ rad, the optimum application height results in about -20, 20 and 60 cm for the eccentricity of vehicle gravity center 0.05, 0.00 and -0.05, respectively.

(3) The optimum effective driving force decreases remarkably with the increment of slope angle due to the increasing vehicle weight component toward the sloped terrain surface, while the amount of sinkage slip ratio relation is almost unchangeable for the slope angle.

(4) The optimum application height of the optimum effective driving force tends to decrease with the increment of eccentricity of vehicle gravity center and slope angle of terrain. For the eccentricity of vehicle gravity center 0.00, the optimum application height for the weak sandy slope terrain of 0, $\pi/18$, $\pi/9$ and $\pi/6$ rad results in about 60, 60, 20

and − 40 cm, respectively.
(5) The automated control system of the optimum application height, i.e. the positioning system of the attachment of tractor could be developed by use of some inclinometer.

REFERENCES

1) T.Muro : Grouser Shape Effect on Tractive Performance of a Flexible Tracked Vehicle Carrying up Slope Terrain, Proc. of 4th North American Regional ISTVS Conference, 1992.
2) T.Muro : Tractive Performance of a Bulldozer Running on Weak Ground, J. of Terramechanics, Vol.26, No.3/4, pp.249-273, 1989.
3) T.Muro : Traffic Performance of a Flexible Tracked Tractor Carrying up and down Weak Slope, SOIL AND FOUNDATIONS, in printing.
4) T.Muro : Optimum Track Belt Tension and Height of Application Forces of a Bulldozer Running on Weak Terrain, J. of Terramechanics, Vol.28, No.2/3, pp.243-268, 1991.
5) T.Muro : Stress and Slippage Distributions under Track Belt Running on a Weak Terrain, SOILS AND FOUNDATIONS, Vol.29, No.3, pp.115-126, 1989.
6) T.Muro : Drawbar Pull Control System of a Flexible Tracked Vehicle of Weak Terrain, Proc. of 6th Int. Sympo. on Automation and Robotics in Construction, pp.260-267, 1989.